International Journal of Innovative Technology and Exploring Engineering (IJITEE)
ISSN: 2278-3075 (Online), Volume-9 Issue-3, January 2020

Dual-Band Parasitic Microstrip Patch Antenna for Wireless Applications

N. Rajesh Kumar, P.D. Sathya

Abstract*: The paper presents a novel dual-band patch working at GSM band and S-band. The patch encompasses a rectangular radiator coupled with a parasitic patch in the coplanar region and a split ring resonator in the ground region. The patch is analyzed numerically and is synthesized using the HFSS simulator. Finally, the performance characteristics of the model are measured and are compared with numerical and simulated results. The patch gives two different bands at 950MHz and 2.3GHz and gives -10dB impedance bandwidth in the lower band from 950MHz -1GHz and higher band from 2.275GHz – 2.325GHz. The patch also accomplishes a gain of 4.74dBi in the effective band 1 and 4.02 dBi in the operating band 2.

Keywords: Dual Band, Energy harvesting, microstrip patch, rectenna, rectifier.

I. INTRODUCTION

Microstrip patches are mostly extensively used in wireless devices due to its less weight, ease of fabrication and better design optimization solutions [1]-[2]. It ranges from linear polarized [3] to circular polarized [4] patches, narrowband to ultra-wideband patches. This patch plays a crucial role in radar systems, satellite communications, military, and airborne communications and remote sensing applications. In general, the patches are fed by different techniques including coaxial fed, aperture coupling [5], microstrip line feed [6], the inset fed, proximity coupling [7], L feed [8] each having different advantages and its limitations. Recently graphene are also used to enhance antenna capabilities [9]. Dual-band patches are much more popular due to their ability to generate a strong signal in two bands which are much required in mobile communications systems. These patches have very sharp dual bands targeting only operating frequencies in the desired applications and also these bands are separated significantly from each other to avoid co-channel interference. These properties make dual-band patches are a stable and easy way to connect with other devices. Most of the paper discussed above lacks numerical analysis of the model and hence there is a need for systematic analysis of the patch model at each stage.

Revised Manuscript Received on January 30, 2020.
***** Correspondence Author
N.Rajeshkumar*, Department of Electronics and Communication Engineering, Annamalai University, Chidambaram, Tamil Nadu, India.
P.D. Sathya, Department of Electronics and Communication Engineering, Annamalai University, Chidambaram, Tamil Nadu, India.

In the proposed work the most widely used rectangular patch is taken and is analyzed step by step through numerical equations to interpret the performance characteristics of the patch. It is then coupled with parasitic patch to induce additional band for wide applications including satellite communications. Further, the work is extended to introduce SRR in the ground surface to enhance the patch performance characteristics. The proposed model is designed to operate at two different operating bands in GSM and S-band standards with sufficient gain characteristics suitable for various applications.

II. PATCH DESIGN PRINCIPLES

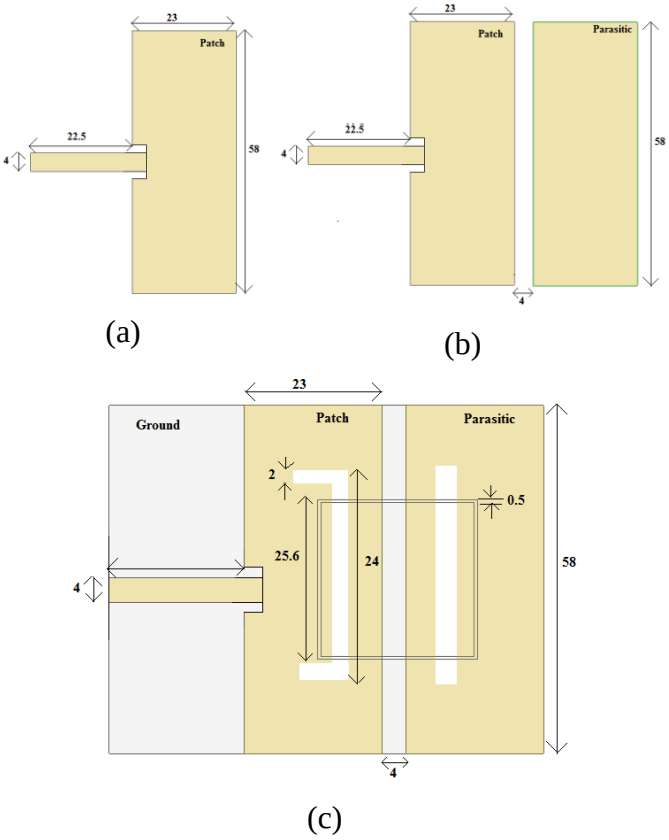

Fig. 1.(a) Rectangular patch patch (b) Rectangular patch patch with a parasitic patch (c) Proposed patch patch with SRR

The patch comprises of three stages. Initially, a simple rectangular patch as exposed in Fig. 1(a) is designed and its performance metrics are analyzed using HFSS. The second stage involves the introduction of a parasitic patch as exposed in Fig. 1(b) with a rectangular patch and its effects over the rectangular patch is studied.

Finally, a slip ring resonator (SRR) is etched on the ground region as exposed in Fig. 1(c) is designed and the overall performance metric is studied. All the three patch models are considered on low loss substrate with a permittivity of 2.65 and a loss tangent of 0.0015 with a thickness of 1.5mm. The entire model is designed on a single-layer substrate to make the patch less complex and feasible to integrate with other RF components. The patch is fed by an inset fed (50ohm) technique to make more control over patch impedance matching.

III. NUMERICAL ANALYSIS

The RLC circuit for a rectangular patch can be realized with RLC components terminated with input impedance Zp as depicted in Fig. 2.

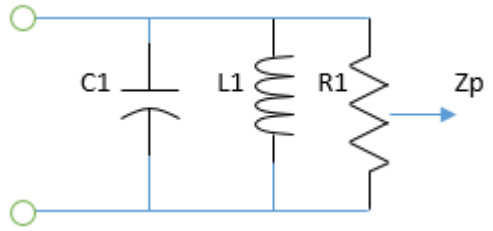

Fig. 2.RLC Circuit of Rectangular patch

The Corresponding RLC values of the radiator can be derived from equations specified below

$$C_1 = \frac{LW\varepsilon_0\varepsilon_e}{2H} COS^2\left(\frac{\pi X_0}{L}\right) \quad (1)$$

$$R_1 = \frac{Q}{\omega_r^2 C_1} \quad (2)$$

$$L_1 = \frac{1}{C_1\omega_r^2} \quad (3)$$

$$Q = \frac{C\sqrt{\varepsilon_e}}{4fH} \quad .$$

Where L, W, H are the Patch length, width, thickness, and X0- feed point location. The permittivity of the medium is taken as εr. The RLC model of parasitic patch coupled with the rectangular radiator is depicted in Fig. 3. The RLC components for the parasitic element is derived as same as rectangular radiator RLC components using equations (1)-(3). The RLC circuit is terminated with an input impedance of Z_{pp}.

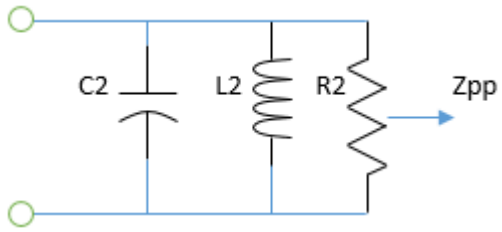

Fig. 3. RLC circuit model for parasitic patch

Between the patch element and the parasitic element, there exists a gap region, which adds a capacitive effect over the patch circuit. The RLC model for the overall capacitance value resulted from the gap region is depicted in Fig. 4 and is derived using equation (4)-(5) given below

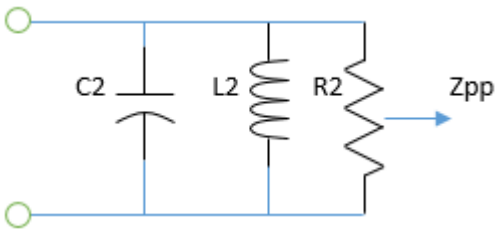

Fig. 4.RLC circuit model for Gap Capacitance

$$C_g = 0.5.H.Q_1 exp\left(-1.86\left(\frac{G}{H}\right)\right)\left[1 + 4.09\left\{1 - exp0.75HW\right.\right. \quad (4)$$

$$C_{p1} = C_L\left(\frac{Q_2+Q_3}{Q_2+Q_1}\right) \quad (5)$$

Where

$$Q_1 = 0.04598\left\{0.03 + \left(\frac{W}{H}\right)^{Q_4}\right\}(0.272 + \varepsilon_r 0.07)$$

.

$$Q_2 = 0.107\left[\frac{W}{H} + 9\right]\left(\frac{G}{H}\right)^{3.23} + 2.09\left(\frac{G}{H}\right)^{1.05} + \left[\frac{1.5+0..3\left(\frac{W}{H}\right)}{1+0..6\left(\frac{W}{H}\right)}\right]$$

.

$$Q_3 = exp(-0.5978) - 0.55$$

.

$$Q_4 = 1.23$$

.

Finally, the RLC circuit model for the feed is depicted in Fig. 5. The line is terminated with impedance ZL. The Land Components of the feed line is derived from equation (6)-(7)

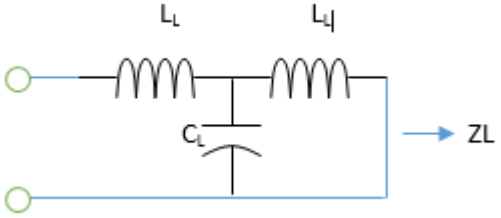

Fig. 5.RLC circuit model for Feedline

$$C_L = C_H\frac{\sqrt{\varepsilon_{eff}}}{Z_0 c}$$

$$C_H = 0.412\left[\frac{(\varepsilon_e+0.3)\left(\frac{W}{H}+0.264\right)}{(\varepsilon_e-0.258)\left(\frac{W}{H}+0.8\right)}\right]$$

$$L_L = 100.H\left(4\sqrt{W_s/H} - 4.21\right)nH \quad (6)$$

$$C_L = W_S\{(9.5\varepsilon_r + 1.25)\,W_s/H + 5.2\varepsilon_r + 7.0\}pF \quad (7)$$

Where CL is the Feedline capacitance and LL is the feed line inductance. The overall RLC model for the proposed patch is depicted in Fig. 6.

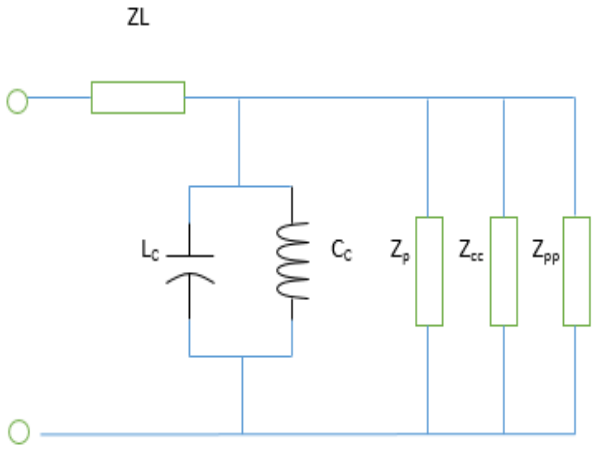

Fig. 6.RLC circuit of proposed model

In general, the resonant frequency is derived from equation (8)

$$f = C/2L_{es}\sqrt{\varepsilon_{re}} \tag{8}$$

Where L_{es} is the effective realized length and ε_{re} is the effective realized permittivity of the substrate or the medium whose value are given below.

$$\varepsilon_{re} = 1/2\left[(\varepsilon_r + 1) + (\varepsilon_r - 1)(1 - 12.H/W_s)^{-1}/_2\right]$$

$$L_{es} = L_s + \Delta L_S$$

$$\Delta L_S = H.0.412\left[\frac{(\varepsilon_{re}+0.3)\left(\frac{W_S}{H}+0.264\right)}{(\varepsilon_{re}-0.258)\left(\frac{W_S}{H}+0.8\right)}\right]$$

The Characteristic impedance $Z_L$and the input impedance Z_{in} of the patch is given in equation (9)-(10) given below.

$$Z_L = j\omega L_L + \frac{1}{j\omega C_L + \frac{1}{j\omega L_L}} \tag{9}$$

$$Z_{in} = Z_L + \frac{1}{\frac{1}{j\omega C_L + \frac{1}{j\omega L_L} + \frac{1}{z_p} + \frac{1}{z_{pp}} + \frac{1}{z_{cc}}}} \tag{10}$$

Based on the above equations, the performance characteristic metric such as reflection coefficient, VSWR and return loss are deduced using the equations given below.

$$\Gamma = \frac{Z - Z_{in}}{Z + Z_{in}}$$

$$VSWR = \frac{1 + \Gamma}{1 - \Gamma}$$

$$R_L = 20\ log\ |r|$$

IV. PARAMETRIC ANALYSIS OF THE PROPOSED PATCH

Analysis of antenna design parametric dimensions is carried to determine the result of design restrictions over patch performance metrics. Fig. 7 depicts the effect of substrate thickness over the patch impedance characters. It is observed that with a rise in antenna substrate thickness moves the operating band (both lower and the upper band) towards higher resonating regions.

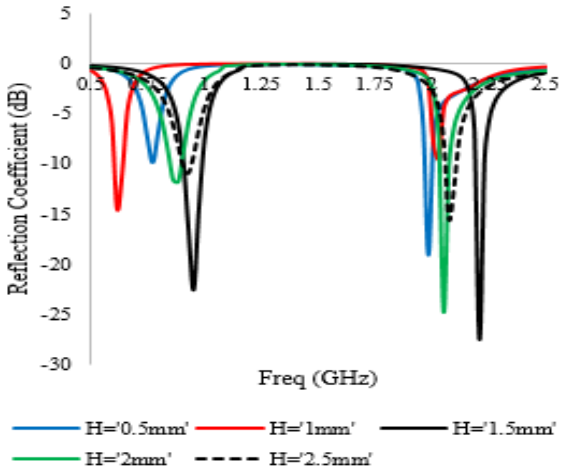

Fig. 7.Effect of substrate thickness (H) on reflection coefficient (dB)

Fig. 8 shows the effect of feed line width (Ws) over the patch impedance bandwidth. It is observed that with a rise in patch substrate thickness moves the operating band (both lower and the upper band) towards lower resonating regions. This is due to the effect of capacitance CL over patch frequency bands as both are directly proportional to each other.

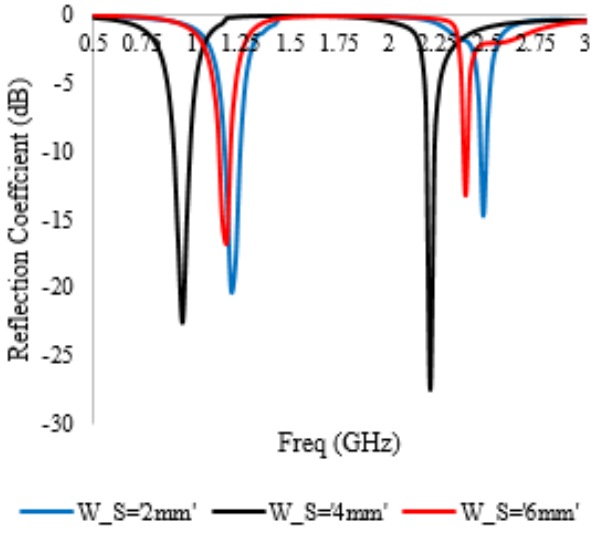

Fig. 8.Effect of feed line width (Ws) over the reflection coefficient (dB)

Fig. 9 shows the result of feed length (Ls) over the patch reflection coefficient. It is observed that with an increase in patch substrate thickness moves the operating band (both lower and the upper band) towards higher resonating regions. This is due to the effect of Ls over patch frequency bands as both are inversely proportional to each other.

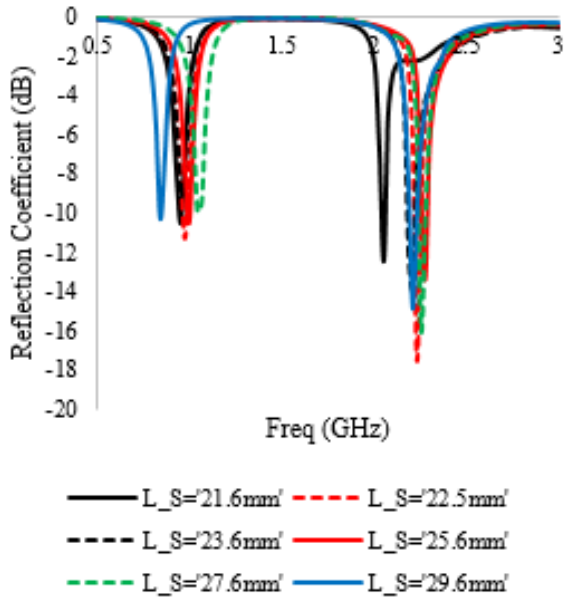

Fig. 9.Effect of feed line length (Ls) over the reflection coefficient (dB)

Fig. 10 shows the effect of the Gap region (G) over the reflection coefficient (dB). It is observed that change in gap regions swings the patch band (both upper and lower band) between two ends of the operating frequency regions.

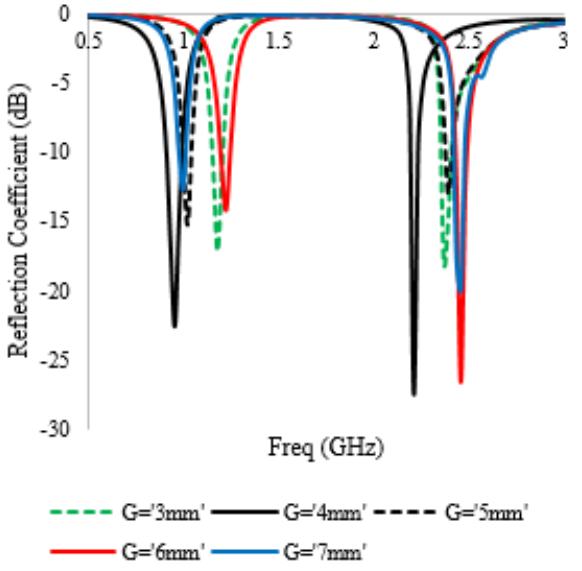

Fig. 10. Effect of Gap region (G) over the reflection coefficient (dB)

V. RESULTS AND DISCUSSIONS

Base on the above equations discussed in numerical analysis and parametric analysis, the RLC values of the patch design are given in Table I.

Table I. Patch design dimensions

Parameter	Specifications
Substrate Height (H)	1.5mm
Permittivity (εr)	2.64
SLoss Tangent (tanδ)	0.0015
Patch width and Parasitic width (W)	23mm
Patch Length and Parasitic Length (L)	58mm
Feedline Length (Ws)	22.5mm
Feedline Width (Ws)	4mm
Gap region (G)	4mm
Notch_width (WN)	2.74
Notch_length(LN)	7.24
SRR thickness (ST)	0.5mm

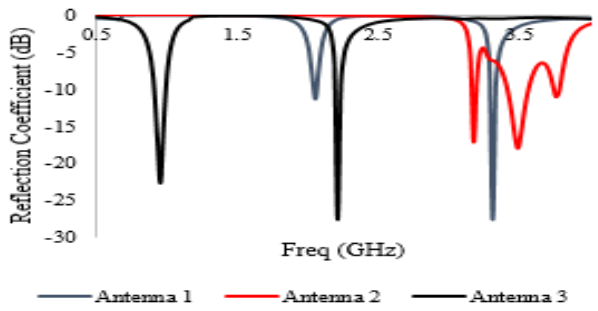

Fig. 11. Comparison of the proposed patch with other patch models.

The proposed patch model is designed using HFSS and is simulated. The resultant output is compared with both numerical and experimental results. Fig. 11 shows the impedance curve for a rectangular radiator patch model with a parasitic model without SRR and proposed a model with SRR. It is witnessed that the patch functions at two different bands at 950MHz and 2.3GHz. The model gives -10dB impedance bandwidth in the lower band from 950MHz -1GHz and a higher band from 2.275GHz – 2.325GHz.

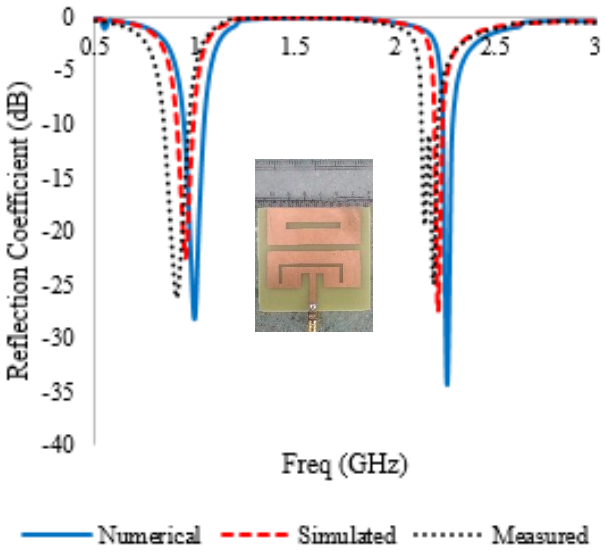

Fig. 12. Impedance characteristics of the patch.

Fig. 12 shows the comparison of -10dB impedance bandwidth curve observed from simulated, numerical and experimental results. It is inferred that the impedance bandwidth curve obtained from simulated, numerical and experimental results is closely matched with each other.

The radiation characteristic of the patch is simulated and are validated. The resultant radiation pattern is given below.

Fig. 13 shows the radiation shape for the E and H plane corresponding to 950 MHZ (Band 1). The plot displays the relationship of both simulated and measured pattern. It is inferred that the patch gives an omnidirectional pattern for the E plane and doughnut shape pattern for the H plane in working band 1 with a gain of 4.74dBi.

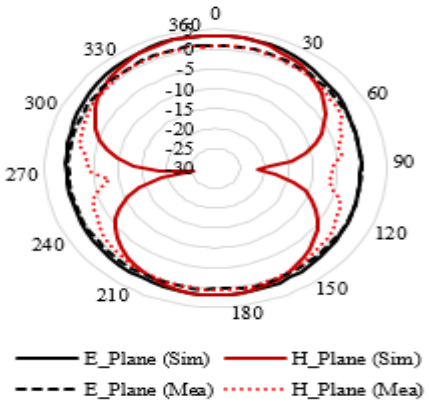

Fig. 13. Radiation pattern for band 1.

Fig. 14 shows the radiation shape for the E and H plane corresponding to 2.3 GHz (Band 2). The plot displays the relationship of both simulated and measured pattern. It is inferred that the patch gives an omnidirectional pattern for E plane and doughnut shape pattern for the H plane in the operating band 2 similar to that of band 1 with a peak gain of 4.02dBi.

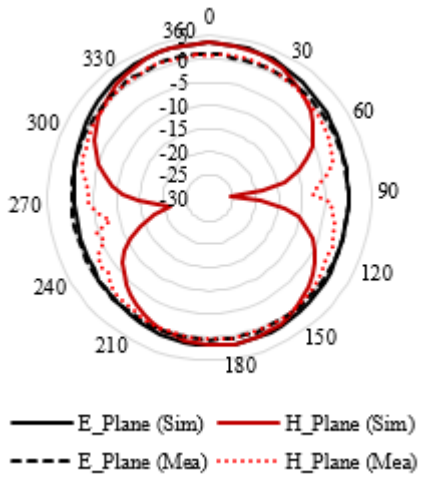

Fig. 14. Radiation pattern for band 2.

VI. CONCLUSION

The paper presents a novel dual-band patch loaded with SRR resonators. The patch is excited by 50-ohm inset fed and is designed on the single-layer substrate. The patch resonates at two different bands at 950MHz and 2.3GHz and gives -10dB impedance bandwidth in the lower band from 950MHz -1GHz and higher band from 2.275GHz – 2.325GHz. The patch also achieves a peak gain of 4.74dBi in the operating band 1 and 4.02 dBi in the operating band 2. The proposed design can be used for modern satellite communication for both uplink and downlink data transfer processes.

REFERENCES

1. I. J. Bahl, S. S. Stuchly, M. A. Stuchly and J. J. W. Lagendijk, "Microstrip Loop Radiators for Medical Applications," in IEEE Transactions on Microwave Theory and Techniques, vol. 30, no. 7, pp. 1090-1093, Jul. 1982.
2. Jinpil Tak, Jaehoon, “Choi Circular-ring patch antenna with higher order mode for on-body communications.” Microwave and Optical Technology Letters, vol. 56, no.7, pp.1543–1547, 2014.
3. D. Punniamoorthy, G. K. Reddy, V. S. Kamadal, G. V. Gopal and K. Poornachary, "Design of patch antenna with omni directional radiation pattern for wireless LAN applications," 2017 International Conference on Recent Innovations in Signal processing and Embedded Systems (RISE), Bhopal, 2017, pp. 70-74.
4. Manavalan Saravanan and Madihally Janardhana Srinivasa Rangachar, “Design of Rhombus-Shaped Slot Patch Patch for Wireless Communications”, Journal of Computer Networks and Communications Vol. 2019, Article ID 5149529, pp. 1- 7.
5. A. R. Parvathy and T. Mathew, "A novel aperture coupled microstrip circular patch antenna for dual band operation," 2017 Progress in Electromagnetics Research Symposium - Fall (PIERS - FALL), Singapore, 2017, pp. 1738-1742.
6. Y. Sung, “Bandwidth enhancement of a microstrip line-fed printed wide-slot patch with a parasitic center patch,” IEEE Trans. Patchs Propag., vol. 60, pp.1712-1217, 2012.
7. H. Son and S. Jeong, "Wideband RFID Tag Antenna for Metallic Surfaces Using Proximity-Coupled Feed," in IEEE Antennas and Wireless Propagation Letters, vol. 10, pp. 377-380, 2011.
8. M. Saravanan and M. J. S. Rangachar, "A novel rectangular radiator patch with double L-probe fed for RADAR altimeter application," 2016 International Conference on Wireless Communications, Signal Processing and Networking (WiSPNET), Chennai, 2016, pp. 1777-1780.
9. M.Ramkumar, “A Compact Graphene Based Nano-Antenna for Communication in Nano-Network,” Journal of the Institute of Electronics and Computer, Vol. 1, no.1, pp.17-27, 2019.
10. G. Kumar and K.P. Ray, Broadband Microstrip Patch, USA, Artech House, 2003.
11. I.J. Bahal and P.Bartia, Microstrip patch antenna, Artech House, 1980.
12. H. A. Wheeler, "Transmission-line properties of parallel strips separated by a dielectric sheet", IEEE Trans. Microwave Theory Tech., vol. MTT-13, pp. 172-175, Mar. 1965.
13. C. K. Aanandan, P. Mohanan and K. G. Nair, "Broad-band gap coupled microstrip antenna," in IEEE Transactions on Antennas and Propagation, vol. 38, no. 10, pp. 1581-1586, Oct. 1990.

AUTHORS BIOGRAPHY

N Rajesh Kumar doing his Ph.D. at Annamalai University, Chidambaram, and Tamilnadu, India. He had two years of teaching experience in VSB engineering College and his interest includes microstrip antennas. .

P.D.Sathya serving as an Assistant professor in the department of ECE at Annamalai University, Chidambaram, and Tamilnadu, India. She had served several years in teaching research and published many papers in peer reviewed journals. Her current research interest comprises of image processing, optimization methods.